Springer

Journal of Mechanical Science and Technology 22 (2008) 1537~1543

Journal of Mechanical Science and Technology

www.springerlink.com/content/1738-494x
DOI 10.1007/s12206-008-0430-9

Optimum design of roll forming process of slide rail using design of experiments

Minjin Oh and Naksoo Kim*

Department of Mechanical Engineering, Sogang University, Seoul, 121-742, Korea

(Manuscript Received December 6, 2007; Revised April 4, 2008; Accepted April 26, 2008)

Abstract

In the design of the roll forming process, design errors can be determined in advance by using an FE simulation tool such as SHAPE-RF. In the case of a product such as a slide rail having a complicated shape and requiring high-precision forming, a standard is necessary for quantitatively evaluating the quality of the formed shape. In the analysis of the roll forming process of a slide rail, the pass having the largest deformation is designated as the target pass and the positions and shapes of the rolls are set as design variables. A minimum number of simulations was performed by using the table of orthogonal arrays. A cost function was obtained from the results by using the design of experiments such as the response surface method and it was minimized for satisfying the design constraints. By improving the design of the target pass, the shape of the final product approaches that intended by the designer.

Keywords: Design of experiments; Finite element method; Roll forming process; Shape difference factor

1. Introduction

Roll forming is a process that progressively bends a flat strip of sheet metal through pairs of forming rolls, and it can be used for inexpensively manufacturing long sheet metal products with a constant cross section. Since roll forming requires manpower only for loading the strip and unloading the product, the manpower required can be reduced. If the shape of the product is simple, it takes little time to change the die and to set up a process. Since the length of the product can be controlled easily, roll forming can also be used for the batch production of small quantities of a product. Since the roll forming process was designed based on the designer's experience for developing a new product or improving the quality of existing products, the design defects were confirmed after the production of the prototype; therefore, the compatibility of the corrected design could be verified after the production of the prototype. This process leads to an increase in the production cost, which reduces the competitiveness of manufacturers. In order to solve this problem, an FE simulation of the roll forming process is used prior to the production of a prototype in order to predict design defects and reduce the cost of design correction.

Bhattacharayya et al. [1] performed a semi-empirical approach and by minimizing the total energy produced an expression for predicting deformation length of a channel section. Duggal et al. [2] compared the FE simulation results with Bhattacharayya's experimental results. And other numerical [3-6] and experimental [7, 8] studies have been performed.

Hong and Kim [9] developed a 3D FEM program for the roll forming process and predicted the scratch defect of the roll forming process with the rigid-plastic finite element method. The analysis using the rigid-plastic finite element method has also been extended to predict the edge shape [10] and roll wear [11]. Kim et al. [12] made the prediction of buckling

*Corresponding author. Tel.: +82 2 705 8635, Fax.: +82 2 712 0799
E-mail address: nskim@sogang.ac.kr

behavior of the roll forming process. Sheikh and Palavilayil [13] assessed an FE simulation program. The effectiveness of research by using the FE simulation tool has been verified by several studies [14-17].

In this research, the accuracy of FE simulation is verified through a comparison of the shape between the simulation and experimental results. The shape difference factor (SDF) is suggested as a standard for quantitatively evaluating the quality of the formed shape. With regard to the analysis of the roll forming process of a slide rail, the pass in which the largest deformation occurs is designated as the target pass. The positions and the curvature of rolls are set for the design variables. The cost function is obtained by using the design of experiments such as the response surface method (RSM), and it is minimized by using the Broyden-Fletcher-Goldfarb-Shanno (BFGS) method. Subsequently, the design is corrected by the minimized result and it causes the shape of the final product to approach that intended by the designer. The proposed method and its complete procedure are described in this paper.

2. Research methods

2.1 Design of experiments

This section describes the scheme of the experiments—how to design experiments to solve a problem, how to record data, and how to obtain the maximum information through the least number of experiments by analyzing the data using some statistical techniques. In other words, the design of experiments selects the parameters of a problem, selects an experimental method, decides the order of experiments, and selects an optimum analysis method. For a design that has many parameters, predictable interactions of two parameters are detected, and information on two or more interactions is sacrificed. As a result, a table is made for an experimental plan with a small number of experiments. The table is called as the "table of orthogonal arrays."

The response surface method (RSM) is mainly used to obtain an explicit function from experimental data. Recently, it has been used to represent a relationship between experimental parameters and responses from numerical experimental values as the explicit function [18]. Two methods can be used to calculate a response surface. First, an approximate function is assumed and the equations of the coefficients of the function are solved numerically to find a relationship between the variables and the function values. Second, the approximation function is evaluated by using an optimization [19].

In this study, a second-order regression model such as that given by Eq. (1) is used to calculate a response surface.

$$y = \beta_0 + \sum_{i=1}^{n_d} \beta_i x_i + \sum_{i=1}^{n_d} \sum_{j \geq i}^{n_d} \beta_{ij} x_i x_j \tag{1}$$

where x_i denotes the design variables; n_d, the number of design variables; and β_i, the unknown coefficients. Eq. (2) is used to calculate the coefficients of RSM that minimize the square summation of the residuals using least square method.

$$\boldsymbol{\beta} = (\mathbf{X}^{\mathrm{T}}\mathbf{X})^{-1}\mathbf{X}^{\mathrm{T}}\mathbf{Y} \tag{2}$$

where $\mathbf{X}$ denotes the design matrix comprising experimental points and $\mathbf{Y}$ denotes the response vector.

2.2 Shape difference factor

If products that are manufactured through the roll forming process do not meet the standards because of a design error, it is necessary to correct the design defects, as shown in Fig. 1.

A slide rail having a complicated shape and requiring high precision in forming and straightness is manufactured by using the roll forming process [20]. It is difficult to determine the compatibility of the design since the product has a complicated shape. A standard is necessary to quantitatively evaluate the quality of the formed shape; one such standard is called the shape difference factor (SDF). In order to quantitatively evaluate the precision of the shape of a

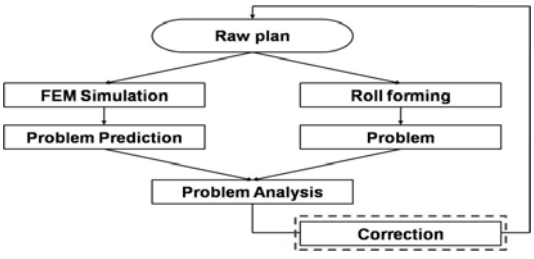

Fig. 1. Flow chart for the correction of the roll forming process design.

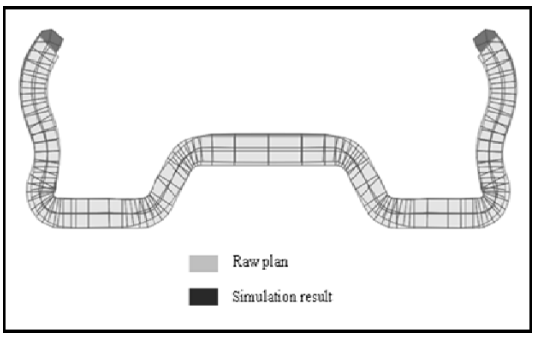

Fig. 2. Comparison of the raw plan and the simulation result.

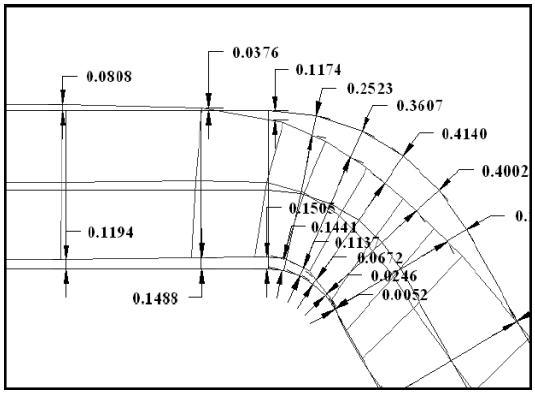

Fig. 3. Measurement of the difference between the raw plan and the simulation result.

product manufactured by the roll forming process, the cross section of a simulation or experimental result is set on the center of the cross section of a raw plan with grids drawn on it, as shown in Fig. 2. As shown in Fig. 3, SDF is decided by the summation of the difference in the distance that is measured between the raw plan and the simulation or experimental result along the direction of thickness and it is defined as given by Eq. (3).

$$\mathrm{SDF} = \sqrt{\sum_{i=1}^{n} (d_i / t_0)^2} \tag{3}$$

where d_i denotes the difference in distance between the result and the raw plan at the i^{th} elements and t_0 denotes the thickness of the initial strip. Since the shape of the cross section of the product is symmetric, the SDF is measured at the right cross section of the product.

3. Simulation and experimental results

3.1 Process condition

A slide rail is comprised of an inner member, middle member, outer member, and bearing balls. Since this research focuses on the slide rail, the middle member is analyzed because an inner rail and an outer rail are formed at the middle member. The middle member is manufactured with a 25-pass line. The distance between the passes is 350 mm; odd-numbered passes are set up as driving rolls, and even-numbered passes are set up as idle rolls, and the velocities of each pass roll are set up to produce a product with a constant velocity of 40m/min.

The thickness and width of the initial strip is 2 mm and 60 mm, respectively; the strip is made of SCP10, whose material properties are listed in Table 1. The final shape of the cross section of the product manufactured in the experiment is shown in Fig. 4.

Table 1. Material properties of SCP10

Young's modulus (GPa)	210
Poisson's ratio	0.3
Yield Strength (MPa)	433
UTS (MPa)	460

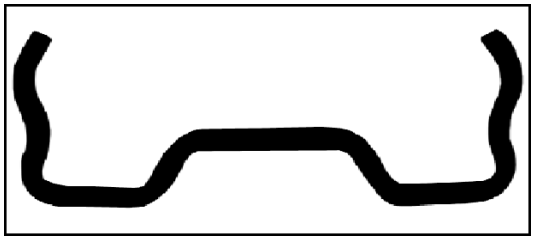

Fig. 4. Cross section obtained from the experiment.

3.2 FE simulation software

FE simulations are performed by the roll forming simulation program SHAPE-RF v4.0.0 based on the rigid-plastic finite element method. This program uses the normalized plane strain condition as the initial boundary condition for initially determining the free surface. The velocity field is calculated by the FEA of the 3D kinematic steady state and the final shape is determined by an iterative method that calibrates the boundary conditions and the free surface. Information such as the strain rate and pressure torque

Table 2. Process conditions of FE simulation.

Flow stress (MPa)	$\sigma_f = 502(0.002+\bar{\varepsilon})^{0.024}$	
Initial thickness (mm)	2.0	
Strip width (mm)	60.0	
Friction coefficient	0.1	
No. of PASS	25	
No. of elements	Section	80
	Rolling direction	20

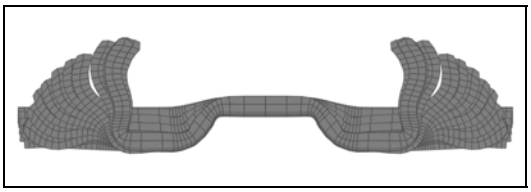

Fig. 5. Flower pattern of the slide rail's middle member.

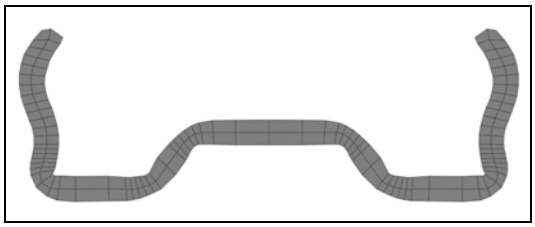

Fig. 6. FE simulation result.

is obtained based on the velocity field. The reliability of SHAPE-RF has been verified by several previous papers [9-13].

The process conditions of the FE simulation are listed in Table 2. Swift's flow stress equation is used to express the stress-strain relation of a strip, and it is defined as given by Eq. (4).

$$\sigma_f = K(\bar{\varepsilon}_0 + \bar{\varepsilon})^n \tag{4}$$

where σ_f denotes the flow stress; K, the strength coefficient; $\bar{\varepsilon}$, the effective strain; $\bar{\varepsilon}_0$, the initial effective strain; and n, the strain hardening coefficient. The flow stress of the strip is obtained by using the "convert" function of SHAPE-RF and it is shown in Table 2. The flower pattern of the middle member is obtained by using the FE simulation program and it is shown in Fig. 5. The final shape of the cross section of the roll forming product is shown in Fig. 6.

3.3 Verification of FE simulation software

The SDF obtained from the experimental and

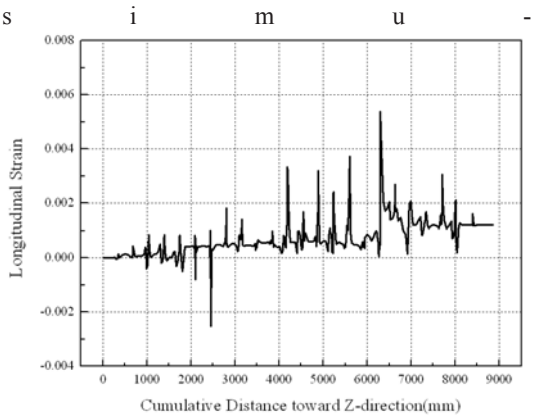

Fig. 7. Longitudinal strain along the rolling direction.

lation results is 0.87450 and 0.91677, respectively. The difference between the results and the raw plan mostly occurs at areas where the slide rail is bent. The relative error is 4.83%.

The FE simulation cannot perfectly approximate the real process because obscure parameters exist at the site of the manufacturing process. For example, for any model of friction that expresses the contact between objects to be valid, it must explain the frictional behavior of two bodies under different loads, speed of relative sliding, temperature, surface conditions, environment, etc., as observed in practice. Consequently, many models have been proposed with varying degrees of success [21]. Although many uncertain parameters exist, as mentioned above, the FE simulation is verified since the shape difference error between the FE simulation and experimental results that is evaluated at the final section increases to 4.83% as compared to the incipient shape.

4. Procedure for design correction and discussion

4.1 Designation of target pass

For design variables to be applied to the design of experiments, they should be restricted because many process variables are found in the roll forming process. In the FE simulation of the roll forming process of the slide rail, the pass where the largest deformation occurs is designated as the target pass for the design variables. The longitudinal strain along the rolling direction is shown in Fig. 7 and the largest deformation occurs at the 6.3 m spot along the rolling direction. Therefore, the 18th pass is designated as the target pass.

Table 3. Levels of the design variables (unit : mm).

Design Variables	Level 0	Level 1	Level 2
A	17.7	18.7	19.7
B	12.5603	13.5603	14.5603
C	5	5.4	5.8

4.2 Table of orthogonal arrays

The strip is bent by the left and right rolls at the 18th pass. Since the slide rail has a symmetric shape, the design variables are limited to the right roll. Design variable A is the *x*-coordinate of the flat part of the right roll and B is the y-coordinate of the same part. C is the curvature of the right roll. The design variables and levels are listed in Table 3 and a table of orthogonal arrays L_9 (3^4) is used. Table 4 shows the table of orthogonal arrays for the SDF obtained from the FE simulation results.

4.3Optimization of the cost function

Based on the table of orthogonal arrays, the cost function obtained by RSM is given by Eq. (5) as:

$$\begin{aligned}\Phi =& 13.90852 - 0.93098 x_1 + 2.62837 x_2 \\ & - 7.13367 x_3 + 0.05303 x_1^2 - 0.03022 x_2^2 \\ & + 1.08379 x_3^2 - 0.08205 x_1 x_2 - 0.37625 x_2 x_3\end{aligned} \tag{5}$$

where x_1 denotes the design variable A; x_2, the design variable B; and x_3, the design variable C.

In order to examine the adequacy of the cost function, Fig. 8 shows the comparison of the values between the cost function in which the conditions of Table 4 are applied and the SDF obtained from the FE simulation results. In order to investigate how the numerical differences in the compared values exist, it is verified through Eq. (6) that the error is less than 1%. Therefore, the cost function can represent the SDF between the final shape of the product and the raw plan when the 18th pass is corrected.

$$\text{Error}(\%) = \frac{\left|\Phi^c - \Phi^a\right|}{\Phi^c} \times 100 \tag{6}$$

where Φ^c denotes the SDF computed from each simulation and Φ^a denotes the value of the cost function when the same variables are inputted.

Table 4. Table of orthogonal arrays for the SDF.

No.	A	B	C	SDF of the simulation
1	0	0	0	1.38007
2	0	1	1	1.07844
3	0	2	2	0.88306
4	1	0	2	1.22510
5	1	1	0	1.35087
6	1	2	1	0.87713
7	2	0	1	1.18833
8	2	1	2	0.91890
9	2	2	0	1.32407

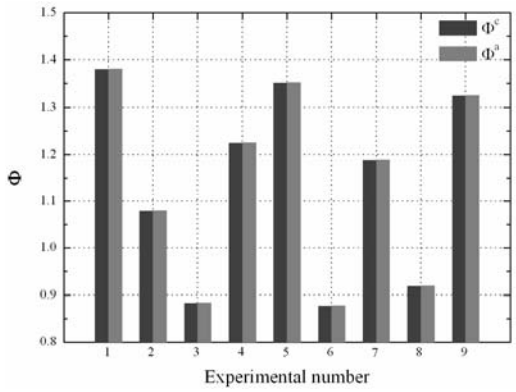

Fig. 8. Comparison of Φ^c and Φ^a

In order to minimize the cost function, the BFGS method, which directly updates a Hessian matrix, is used. Initial design variables and the constraints are given as follows:

$$x_1 = 17.0,\ x_2 = 12.0,\ x_3 = 5.5 \tag{7}$$

$$\begin{aligned} 17.7 \le x_1 \le 19.7 \\ 12.5603 \le x_2 \le 14.5603 \\ 5.0 \le x_3 \le 5.8 \end{aligned} \tag{8}$$

The result of minimization is given as follows:

$$x_1 = 19.7,\ x_2 = 14.5603,\ x_3 = 5.71$$

$$\Phi = 0.60159$$

Based on this result, the 18th pass is corrected and the FE simulation is performed. There is a difference of 30.87 % between the minimum value of the cost function and the SDF of the FE simulation result of

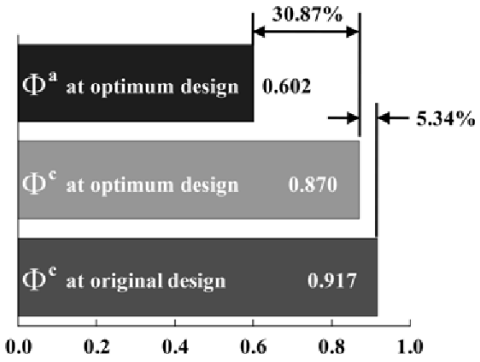

Fig. 9. Comparison of the SDF between the original design and the optimum design.

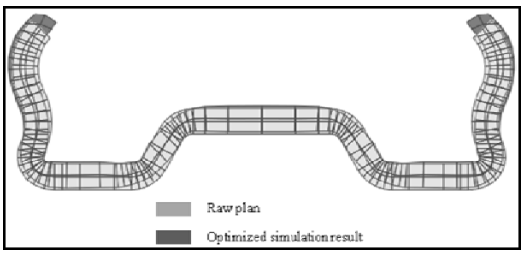

Fig. 10. Comparison of the raw plan and the optimized simulation result.

0.87023. Although the result indicates a wide gap in the minimum of the cost function, the SDF of the optimized result decreases by 5.34 % as compared to the original result of 0.91677; the comparison of the results is shown in Fig. 9. The cross section of the optimized simulation result and the raw plan are compared, as shown in Fig. 10. A significant difference is observed between Φ^c and Φ^a since the cost function obtained from the restricted design variables does not consider all conditions of the target pass such as the design of the top and bottom rolls. Further, roll forming has many design variables such as roll velocities, friction condition, and angle of roll. If more process variables are contained in the design variables, then the error between the FE simulation result and the cost function will be smaller than that in the above result.

5. Conclusions

In order to improve the efficiency of the roll forming process, it is very important to immediately correct a design that has some defects. There is a product called a slide rail that has a complex shape and whose design is difficult to modify. In this paper, the roll forming design was corrected by the design of experiments. The SDF was also introduced to determine the compatibility of the roll design. The conclusions drawn from this study are listed below.

The correction of the design of the target pass, which is designated through the measurement of the longitudinal strain along the rolling direction of the entire process, affects the final shape of the roll forming product.

The SDF, which represents the difference between the cross section of the product that is affected by the change of the design variables and the raw plan, is suggested as a standard. Further, the cost function that can evaluate the SDF is derived by using the design of experiments such as the RSM. The optimum design is determined through the minimization of the cost function. The minimum value of the cost function is applied to the design of the target pass and it decreases the SDF by 5.34 %. Consequently, the cross-sectional shape of the slide rail obtained by the simulation approaches the shape intended by the designer.

Nomenclature

x_i : Design variable
d_i : Difference between the simulation or experimental result and the raw plan
t_0 : Thickness of initial strip
Φ : Cost function
σ_f : Flow stress
$\bar{\varepsilon}$: Effective strain
$\bar{\varepsilon}_0$: Initial effective strain
Φ^c : Computed shape difference factor
Φ^a : Analytical shape difference factor

References

[1] D. Bhattacharayya, P. D. Smith, C. H. Yee and I. F. Collins, The prediction of Deformation length in cold roll forming, *J. Mech. Working Technol.,* 9 (1984) 181-191.

[2] N. Duggal, M. A. Ahmetoglu, G. L. Kinzel and T. Altan, Computer aided simulation of cold roll forming-a computer program for simple section profiles, *J. Mater. Proc. Technol.,* 59 (1996) 41-48.

[3] M. Brunet and S. Ronel, Finite element analysis of roll-forming of thin sheet metal, *J. Mater. Proc. Technol.,* 45 (1994) 255-260.

[4] M. Brunet, B. Lay and P. Pol, Computer aided design of roll-forming of channel sections, *J. Mater. Proc. Technol.,* 60 (1996) 209-214.

[5] C. Liu, Y. Zhou and W. Lu, Numerical simulation of roll-forming by B-spline finite strip method, *J. Mater. Proc. Technol.,* 60 (1996) 215-218.

[6] M. Farzin, M. S. Tehrani and E. Shameli, Determination of buckling limit of strain in cold roll forming by the finite element analysis, *J. Mater. Proc. Technol.,* 125-126 (2002) 626-632.

[7] S. M. Panton, J. L. Duncan, S. D. Zhu, Longitudinal and shear strain development in cold roll forming, *J. Mater. Proc. Technol.,* 60 (1996) 219-224.

[8] M. Lindgren, Experimental investigations of the roll load and roll torque when high strength steel is roll formed, *J. Mater. Proc. Technol.,* 191 (2007) 44-47.

[9] S. Hong and N. Kim, Study on scratch defect of roll forming process, *Trans. of the KSME* (A). 25 (2001) 1213-1219.

[10] S. Lee and N. Kim, Prediction and design of edge shape of initial strip for thick tube roll forming using finite element method, *Trans. of the KSME* (A). 26 (2002) 644-652.

[11] B. Kang and N. Kim, A study on roll wear in the roll forming process, *Trans. of the KSME* (A). 27 (2003) 644-652.

[12] Y. Kim, J. Kim, Y. Jeoung and N. Kim, Buckling analysis of roll forming process using finite element method, *Trans. of the KSME* (A). 27 (2003) 1451-1456.

[13] M. A. Sheikh and R. R. Palavilayil, An assessment of finite element software for application to the roll-forming process, *J. Mater. Proc. Technol.* 180 (2006) 221-232.

[14] A. Alsamhan, P. Hartely and I. Pillinger, The computer simulation of cold-roll-forming using FE methods and applied real time re-meshing techniques, *J. Mater. Proc. Technol.,* 142 (2003) 102-111.

[15] A. K. Datta, G. Das, P. K. De, P. Ramachandrarao and M. Mukhopadhyaya, Finite element modeling of rolling process and optimization of process parameter, *Material Science and Engineering* (A). 426 (2006) 11-20.

[16] M. Lindgren, Cold roll forming of a U-channel made of high strength steel, *J. Mater. Proc. Technol.,* 186 (2007) 77-81.

[17] R. S. Senanayake, I. M. Cole and S. Thiruvarudchelvan, The application of computational and experimental techniques to metal deformation in cold roll forming, *J. Mater. Proc. Technol.,* 45 (1994) 155-160.

[18] E. Kim, I. Lee and B. Kim, Optimum design of washing machine flange using design of experiment, *Trans. of the KSME* (A). 31 (5) (2007) 601-608.

[19] D. Lee, S. Baek, K. Lee, S Cho and W. Joo, Multi-objective optimization in discrete design space using the design of experiment and the mathematical programming, *Trans. of the KSME* (A). 26 (10) (2002) 2150-2158.

[20] S. Jeong, S. Lee, G. Kim, J. Kim and S. Shin, Rigid-plastic finite element method for development mold of dishwasher's under rail roll forming, *Trans. of the KSMPE* Annual Meeting. (2006) 644-652.

[21] S. Kalpakjian and S. R. Schmid, Manufacturing processes for engineering materials, second ed. Addison-Wesley Publishing Company, New York, USA, (1992).